MELTING AND CRYSTALLIZATION OF POLY(OXYETHYLENE) MIXTURES

Ivo LAPES[a], Josef BALDRIAN[a], Jan BIROS[a], Julius POUCHLY[a] and Hanes MIO[b]

[a] *Institute of Macromolecular Chemistry, Academy of Sciences of the Czech Republic, 162 06 Prague 6, Czech Republic*

[b] *Institute of Biophysics and Structure Research, Austrian Academy of Science, Steyergasse 17, A-8010 Graz, Austria*

Received February 21, 1995
Accepted June 23, 1995

Dedicated to Dr Blahoslav Sedlacek on the occasion of his 70th birthday.

Solid–liquid eutectic phase diagrams of mixtures of poly(oxyethylene) (M.w. 2 000) with hydroxy and methoxy endgroups, crystallizing in extended-chain macroconformation only, with glutaric acid, benzoic acid or 1,2-diphenylethane are given. The composition dependence of the melting temperature can be fitted by the Flory–Huggins equation. Interaction parameters χ and interaction energy densities B evaluated from the diluent branch of the phase diagram are consistent with those obtained from the polymer branch provided the calorimetric value of enthalpy of polymer fusion is used in the latter computation. Measurements of small- and wide-angle X-ray scatterings showed a stacked lamellar structure of POE. Below the eutectic melting point, the long period of the polymer is almost independent of the diluent concentration. On raising temperature gradually from this melting point to the melting point of pure polymer, the increasing long period indicates the penetration of the diluent between the lamellae. As follows from SAXS measurements, the crystallinity of poly(oxyethylene) in the mixtures remains unchanged compared to that of the pure polymer.

The investigation of solid–liquid equilibria in polymer systems is of interest from both the morphological and thermodynamic points of view. For a binary mixture of a polymer with a low-molecular-weight diluent (both crystallizable), the melting behaviour can be described by a simple phase diagram with eutectic, provided that the components are miscible in all proportions in the liquid state and neither crystalline complexes nor solid solutions are formed. If the two components do not differ too much in their melting points, both branches of the phase diagram are well developed. This type of behaviour was reported with the mixtures of poly(oxyethylene) with glutaric acid[1], trioxane[2] and water[3,4] of polyethylene with perhydrotriphenylene[5], hexamethylbenzene[6], 1,2,4,5-tetrachlorobenzene[6], 1,3,5-tribromobenzene[7], of polypropylene with pentaerythrite tetrabromide[8] and 1,2,4,5-tetrachlorobenzene[9], and of poly(ε-caprolactone) with trioxane[10].

Most of these studies were performed with high-molecular-weight polymers forming, as a rule, folded-chain crystals. Crystals of this type have lower and history-dependent melting temperatures unlike thermodynamically stable extended-chain crystals. Therefore, the polymer melting branch of the phase diagram may deviate markedly from that predicted by equilibrium thermodynamics[11]. Usually, tedious and not very reliable extrapolations to equilibrium conditions are necessary. Also the morphology of folded-chain crystals is depended on their history.

To avoid these problems we turned our attention to poly(oxyethylene) (POE) fractions of low molecular weight, which are known to form only extended-chain crystals[12]. In this work we report a study of POE of molecular weight 2 000 with two different types of end groups, namely with terminal hydroxy groups (HO-POE) and methoxy groups (MeO-POE). In presence of a crystallizable diluent, we obtained the phase diagram using a DSC calorimeter and determined the crystalline parameters by X-ray diffractometry. The diluents were benzoic acid and glutaric acid; in addition, mixtures of HO-POE with 1,2-diphenylethane were studied by calorimetry. Structural observations of the above systems revealed some new features. In the thermodynamic part, the problems of consistent evaluation of the two branches of the phase diagram were analyzed.

EXPERIMENTAL

Poly(oxyethylene) (M.w. 2 000) with hydroxy or methoxy endgroups (Fluka) was kept in a desiccator and used as received. Benzoic acid (Lachema Brno) was of analytical grade purity. Glutaric acid (Reachim, Moscow), was purified by double precipitation from 30% solution in diethyl ether with a tenfold volume of petroleum ether. The calorimetrically determined purity of both acids exceeded 99.9%. 1,2-Diphenylethane was purified by a column distillation; a middle fraction of purity higher than 99.9% determined by calorimetry and gas chromatography was used.

Preparation of Samples

The solutions were prepared by introducing weighed amounts of the components into 2-ml ampoules. The contents of the sealed ampoules were homogenized above the melting point of the mixture. The solid samples (about 3–5 mg) were hermetically closed in aluminium pans for DSC experiments or sealed in standard glass capillaries for X-ray measurements (1.5–2 mm diameter, wall thickness 0.01 mm). The operations were done in a dry bag under a stream of dry nitrogen to avoid contamination by atmospheric moisture. Simultaneous SAXS and WAXS (SWAX) measurements were performed in vacuum. Before X-ray measurements, the samples were annealed at 90 °C for 1 h and then cooled to room temperature.

Methods

DSC. A DSC-2 Perkin–Elmer apparatus was used for the measurements of melting temperatures (heating rate 1.25 K/min was used to minimize the thermal lag and superheating). The melting point (i.e. the equilibrium liquidus temperature) which corresponds to the maximum of the melting peak was taken. The melting points of pure substances as well as those in the mixtures were independent

of the thermal history, whether they were crystallized isothermally about 20 to 30 K below the melting point of a pure component or dynamically when cooled at a rate from 0.31 to 20 K/h.

WAXS. A HZG4A (Prazisionmechanik Freiberg, Germany) powder diffractometer for wide-angle X-ray diffraction at room temperature was used.

SAXS. A Kratky camera (Paar, Graz, Austria) with a high-temperature unit for measurement of small-angle X-ray scattering curves was used. For step-by-step measurements at elevated temperatures, samples were kept for 30 min to reach the equilibrium state and then the scattering curves were measured.

SWAX. Simultaneous SAXS and WAXS experiments on the mixtures were performed with the SWAX system designed and constructed at Graz[13]. An X-ray tube with rotating anode (Rigaku – Ru200) was used. The scattered CuKα radiation was recorded with two position-sensitive gas detectors in SAXS (1–100 nm) and WAXS (0.34–0.49 nm) regions.

WAXS and SAXS curves were evaluated[14] with profile analysis program FIT. Correction of wide-angle reflections for instrumental broadening was made with the help of Si sample. SAXS curves were desmeared using program[15] DESMGLAT and Lorentz-corrected before evaluation.

RESULTS

Phase Equilibria

From the independence of the melting temperatures on the crystallization conditions we can infer that the chains crystallize only in the extended-chain macroconformation. Some of the thermograms are displayed in Fig. 1. The solid–liquid phase diagrams of the binary mixture of HO-POE with glutaric acid, benzoic acid or 1,2-diphenylethane are shown in Figs 2–4. The mixtures of MeO-POE with the same substances afford the same diagrams.

The dependence of the melting point (i.e., of the equilibrium liquidus temperature) on composition can be described by equations derived from the Flory–Huggins theory[16]. For melting of the low-molecular-weight component (*1*) in mixture with polymer (*2*) we have:

$$\frac{1}{T_{\mathrm{m},1}} - \frac{1}{T^0_{\mathrm{m},1}} = -\frac{R}{\Delta H_1}\left[\ln \phi_1 + (1 - 1/r_2)\,\phi_2 + \chi_1 \phi_2^2\right] \qquad (1)$$

and for melting of the polymer in presence of a diluent

$$\frac{1}{T_{\mathrm{m},2}} - \frac{1}{T^0_{\mathrm{m},2}} = -\frac{R\,V_{2\mathrm{u}}}{\Delta H_{2\mathrm{u}}\,V_1}\left[\frac{\ln \phi_2}{r_2} - (1 - 1/r_2)\,\phi_1 + \chi_2 \phi_1^2\right] . \qquad (2)$$

Here, $T_{\mathrm{m},i}$ is the melting point of a component $i (i = 1, 2)$ in the mixture, the superscript ^{0} refers to the pure component, ϕ_i is the volume fraction of component i in the equilibrium liquid, r_2 is the number of segments per polymer chain, defined as the ratio of

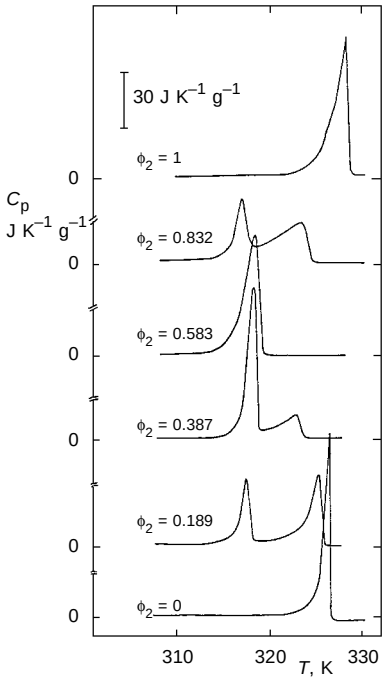

FIG. 1
DSC thermograms of the 1,2-diphenylethane–HO-POE mixtures; ϕ_2 volume fraction of polymer

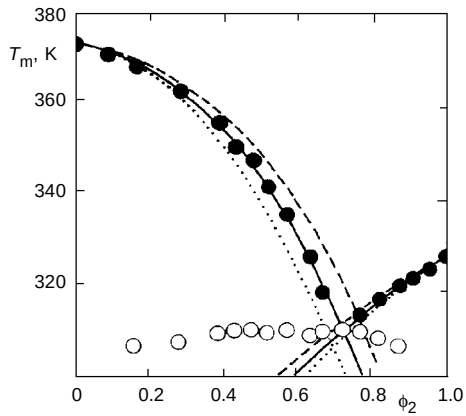

FIG. 2
Phase solid–liquid diagram of the glutaric acid (1)–HO-POE (2) mixture. Symbols (●), (○) denote melting points of the components and eutectic, respectively. Curves $T_m = T_m(\phi_2)$ were calculated using Eqs (*1*) and (*2*) for χ = –2.0 (· · ·), χ = –1.5 (———) and χ = –1.0 (– – – –)

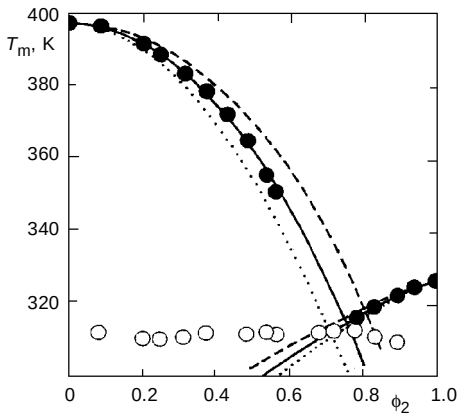

FIG. 3
Phase solid–liquid diagram of the benzoic acid (1)–HO-POE (2) mixture. (For symbols and curves, see Fig. 2.) χ = –1.55 (· · ·), χ = –1.05 (———) and χ = –0.55 (– – – –)

molar volumes V_i of polymer and diluent, $r_2 = V_2/V_1$, ΔH_i is the molar enthalpy of fusion of component i, χ is the Flory–Huggins interaction parameter. The parameter χ_i (i = 1, 2) relates to the melting equilibrium of component i. Subscript u refers to one mol of monomeric unit.

From the course of the function $T^0_{m,i} = f(\phi_2)$, the parameter χ_i (i = 1, 2) can be computed. The interaction parameters χ_1 and χ_2 have been evaluated by a linearization procedure based on rearrangement of Eqs (*1*) and (*2*):

$$-(\Delta H_1/R)\left(\frac{1}{T_{m,1}} - \frac{1}{T^0_{m,1}}\right) - \ln \phi_1 - (1 - 1/r_2)\phi_2 = \chi_1 \phi_2^2 \qquad (3)$$

$$-\Delta H_{2u} V_1 \left(\frac{1}{T_{m,2}} - \frac{1}{T^0_{m,2}}\right) / RV_{2u} - \frac{\ln \phi_2}{r_2} - (1 - 1/r_2)\phi_1 = \chi_2 \phi_1^2 \ . \qquad (4)$$

The left-hand side of Eq. (*3*) or (*4*) was dealt with as a function of ϕ_2^2 or ϕ_1^2, respectively. In this way the χ parameters are taken as temperature-independent, at variance with both theory and experience. Following the original definition of χ, one can introduce[17]:

$$\chi = BV_1/RT \qquad (5)$$

with constant B, the density of interaction energy. We computed B_1 and B_2 in a similar way as χ. The thermodynamical values necessary to evaluate the above equations are given in Table I.

The values of χ_1 and B_1, as calculated from the diluent branch of the coexistence curve, are given in Table II. In evaluation of the polymer branch for a sufficiently high

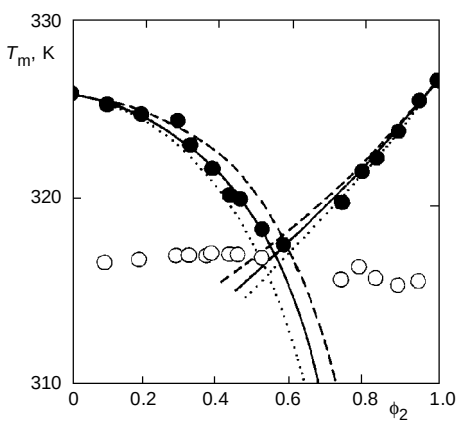

FIG. 4
Phase solid–liquid diagram of the 1,2-diphenylethane (1)–HO-POE (2) mixture. (For symbols and curves, see Fig. 2.) χ = 0.20 (· · ·), χ = 0.35 (———) and χ = 0.50 (– – – –)

polymer molecular weight, ΔH_{2u} is the enthalpy of melting of a perfect crystal with infinitely long chains (for POE the most appropriate value is considered[21] to be 8.7 kJ/mol). In our case (M.w. 2 000), the end effects may play a significant role, and the choice of the ΔH_{2u} is an open problem. Therefore we computed χ_2 or B_2 for various values of melting enthalpy and by interpolation we found ΔH_{2u} for which $\chi_1 = \chi_2$ or $B_1 = B_2$.

As can be seen from Table II, the consistency of χ_1 with χ_2 is achieved using melting enthalpy values which are close to those determined calorimetrically (Table I) rather than to the limiting value for perfect crystals. Hodge et al.[7] came to a similar conclusion with the system polyethylene–1,3,5-tribromobenzene. The sensitivity of our evaluation of interaction parameters is illustrated by curves computed for various values of χ_1 and χ_2 (with ΔH_{2u} = 7.5 kJ/mol) in Figs 2–4.

Our condition of consistency, expressed by $\chi_1 = \chi_2$, might be questioned. The interaction parameter χ is temperature-dependent and the temperature ranges of melting are not the same for the diluent and the polymer. However, our conclusions on the proper choice of ΔH_{2u} have been confirmed by our computation of B_1 and B_2 based on the assumption $\chi \approx 1/T$ (Table II), and also by a modified calculation where we put $\chi = a$

TABLE I
Thermodynamical data of used compounds

Compound	d^a, g cm^{-3}	ΔH_m, kJ mol^{-1}	T_m, K
HO-POE	1.096	7.5	327.0
MeO-POE	1.086	7.5	327.0
Glutaric acid	1.210 (ref.[18])	21.8	372.5
Benzoic acid	1.083 (ref.[19])	16.5	396.8
1,2-Diphenylethane	0.995 (ref.[20])	15.6	325.0

[a] In the liquid state at T_m.

TABLE II
Values of χ_1, B_1 and enthalpies of fusion of HO-POE for $\chi_1 = \chi_2$ and $B_1 = B_2$

Diluent	χ_1	B_1, J cm^{-3}	ΔH_{2u}, kJ mol^{-1}	ΔH_{2u}, kJ mol^{-1}
Glutaric acid	–1.49	–37.9	7.4	7.5
Benzoic acid	–1.05	–31.5	7.3	7.8
1,2-Diphenylethane	0.34	5.7	7.4	7.2

+ b/T. In the latter procedure, a and b are computed from the diluent branch; using these values, an average $\overline{\chi}_2$ parameter (for the temperature range from the eutectic temperature T_E to $T^0_{m,2}$) is predicted and compared with the χ_2 value evaluated directly using Eq. (*4*). The neglection of the composition dependence of the interaction parameter may be more consequential for two reasons: (i) unlike the temperature intervals of the two branches, their composition intervals do not overlap, (ii) if χ_1 depends on ϕ_2, the relation $\chi_1(\phi_2) = \chi_2(\phi_2)$ is invalid. For example, if we put $\chi_1(\phi_2) = \alpha + \beta\phi_2$, then the condition of consistency is $\chi_2(\phi_2) = \chi_1(\phi_2) + \beta/2$ and analogous relations also hold for B_1 and B_2. On the basis of modified Eq. (*3*), we evaluated α and β from the diluent branch and then proceeded in an analogous way as described above for the case of temperature-dependent χ. It was found again that the enthalpy of fusion close to the experimental value ΔH_{2u} = 7.5 kJ/mol performs better in Eqs (*3*) and (*4*) than the perfect crystal value.

The phase diagrams of MeO-POE with diluents were treated in the same way as those of HO-POE. The superiority of the calorimetric ΔH_2 to the ideal value was confirmed in this case, too.

WAXS and SAXS

By means of diffraction methods, the structure of mixtures in two different regions of phase diagrams were studied, namely in the region of solid mixture and in the region where polymer is in solid state and the second phase is liquid.

Solid Mixtures

Figure 5 shows the small-angle scattering curves of MeO-POE mixtures with benzoic acid at various compositions. Scattering curves with a series of maxima reflect the stacked lamellar structure of MeO-POE. The second crystalline component, the acid,

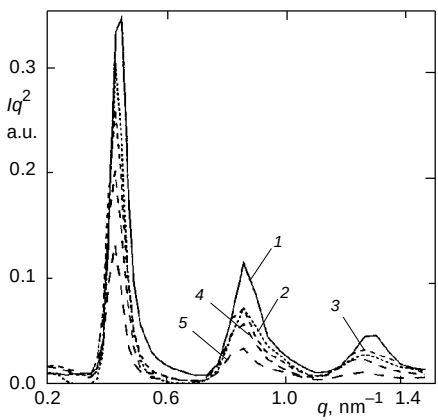

FIG. 5
SAXS curves of MeO-POE–benzoic acid mixtures of various compositions. Mass fraction of POE: *1* 1.00, *2* 0.95, *3* 0.84, *4* 0.76, *5* 0.70

does not contribute to the scattering in the measured interval. Intensities of SAXS reflections decrease with decreasing content of MeO-POE in the mixture.

The structural parameters of MeO-POE–benzoic acid mixture as obtained from SAXS curves are summarized in Table III. Long periods, obtained for pure polymer, i.e. 14.1 nm for MeO-POE and 13.1 nm for HO-POE, correspond to the extended-chain lamellar structures. The positions of scattering maxima of mixtures do not change with composition. In all the mixtures studied, a small shift of low-angle maxima was observed corresponding to an increase of the long period by about 0.3 nm in comparison with pure MeO-POE and HO-POE. The shift is so small that it does not prove the penetration of acids into the interlamellar layers of POE. The effect might be associated with slower crystallization of POE in the mixtures, which enables better development of extended-chain lamellae. We conclude that the acid molecules are not probably present within the interlamellar regions below the eutectic melting point.

For the ideal lamellar model, the relation for the ratios of integral intensity I_n of the n-th order reflection to that of the first order is[22]

$$I_n/I_1 = \frac{\sin^2(n\pi\varphi)}{n^2\sin^2(\pi\varphi)} \ , \qquad (6)$$

where φ is the crystallinity of the system. The crystallinities φ obtained from these ratios are not dependent on composition for the mixtures studied, as shown in Table III. This means that the crystallinity of POE in the mixtures is equal to that of pure POE.

TABLE III
SAXS structure parameters of MeO-POE–benzoic acid mixtures at 20 °C

w_{POE}	Long period, nm, reflection order			Crystallinity[a] from	
	1st	2nd	3rd	I_2/I_1	I_3/I_1
1.00	14.1	7.2	4.9	0.75	0.77
0.95	14.5	7.1	4.9	0.78	0.76
0.84	14.3	7.1	4.9	0.78	0.79
0.76	14.3	7.4	5.0	0.74	0.77
0.70	14.6	7.4	5.0	0.75	0.75

[a] Equation (*6*).

All these facts show that the polymer and acids in the solid state mixtures crystallize independently of each other.

Partly Molten Mixtures

As follows from phase diagrams (Figs 2–4), between the temperature region of solid mixtures with complete phase separation and that of the homogeneous melt mixture, there is a temperature interval of coexistence of liquid and solid phases. In this intermediate region, between the melting temperature of eutectic and that of polymer, the structure behaviour of mixtures was studied. Convenient concentration of POE in mixtures for these studies is around 80 wt.%. We measured the SAXS and WAXS of three mixtures: MeO-POE–benzoic acid with weight fraction $w_{POE} = 0.84$, HO-POE–glutaric acid with $w_{POE} = 0.80$ and HO-POE–benzoic acid with $w_{POE} = 0.85$.

Figure 6 shows the changes of WAXS pattern of HO-POE–benzoic acid mixture for diffraction angles 2θ between 18 and 26° with temperature increasing from 38 to 50 °C, in comparison with the diffraction curve of the solid mixture at room temperature. The series of diffraction patterns reveal the gradual decrease in intensities of crystalline reflections of POE with increasing temperature. For temperatures higher than 47 °C, POE was completely molten and scattering of the crystalline phase disappeared.

Structure parameters obtained from WAXS pattern analysis are summarized in Fig. 7. The integral intensity of the 120 reflections of POE (Fig. 7*a*) decreases with increasing temperature. The crystalline phase of POE dissolves gradually in liquid acid with approaching its melting temperature, in accordance with the phase diagram (Fig. 2).

The apparent crystal size L_{120} of POE in the direction perpendicular to the (120) crystal plane can be determined using the Scherrer equation[23]

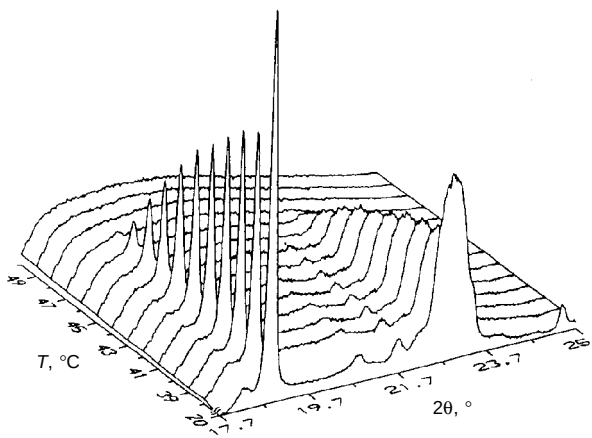

FIG. 6
Temperature changes of WAXS pattern of HO-POE–benzoic acid mixture (w_{POE} = 0.85) measured in the SWAX system

$$L_{120} = K\lambda/\beta_0 \cos\theta \ , \qquad (7)$$

where β_0 is the half-width of the reflection corrected for instrumental broadening and K is approximately unity. Care must be taken in interpretation of this parameter because broadening of reflections may also be influenced by lattice distortions. In the calculation of L_{120} no correction for lattice distortions was applied due to the lack of well detectable higher-order reflections necessary for this correction.

Crystallographic planes (120) of POE are oriented parallel to the polymer chains. The parameter L_{120} therefore characterizes besides lattice distortions the mean lateral size of POE lamellae. This value has a maximum in the measured temperature interval (Fig. 7*b*). The crystalline structure of POE lamellae can hardly improve in the measured temperature interval, where POE gradually dissolves and starts to melt. Therefore the initial increase of the parameter L_{120} reflects mainly the growth of mean lateral dimensions of lamellae. This fact could be explained by preferential dissolution of small-size crystallites, which shifts their mean size to higher values. At higher temperatures, where this value decreases, dissolution and melting of lateral lamellar walls dominated. The lamellar thickness cannot change during heating because the used POE exists only in the extended-chain macroconformation in the crystalline phase.

Figure 8 shows temperature changes of the 1st-order SAXS reflection for the HO-POE–benzoic acid mixture. Changes of SAXS curves with temperature are similar for all the studied mixtures. The higher-order maxima, existing on SAXS curves of solid mixtures (Fig. 5) disappeared for all temperatures in the region of partly molten mix-

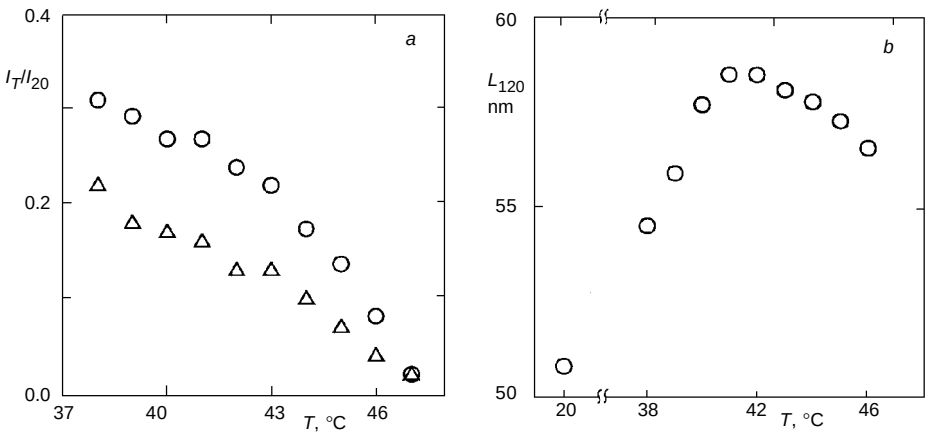

FIG. 7

Temperature changes of structure parameters of HO-POE–benzoic acid mixture (w_{POE} = 0.85); *a* integral intensity of the WAXS 120 reflection (○) and 1st-order SAXS reflection (Δ), *b* apparent crystallite size L_{120}

ture. Integral intensity of the 1st-order SAXS reflection decreased with increasing temperature similarly to the WAXS intensity of the 120 reflection (Fig. 7*a*) and confirmed the gradual dissolution and melting of the POE lamellae when the temperature is approaching the melting point of POE in the mixture.

The long periods in solid mixtures were determined to be 14.5 nm and 13.4 nm for MeO-POE and HO-POE, respectively. These values increase with increasing temperature (Fig. 9). In the vicinity of melting temperature of polymer in mixture the long periods reach value 15.6 nm for the HO-POE–benzoic acid, 17.1 nm for MeO-POE–benzoic acid and 16.3 nm for HO-POE–glutaric acid mixtures (Fig. 9). Since the used POE only forms extended-chain lamellae, this growth of the long period means that liquid phase (i.e., mixture of POE with acids) penetrates between the POE lamellae in the stacks. Similar increase of long periods was observed by Terrisse et al.[24] for mixtures of POE 2000 with liquid oligomers POE 300 and POE 400. The lamellar structure of pure POE revealed lower sensitivity to temperature (Fig. 9) – the growth of long period is much smaller and the 2nd-order maximum of the SAXS was preserved up to the melting point of POE.

DISCUSSION

Strongly negative values of the interaction parameter χ in mixtures of POE with glutaric or benzoic acids (Table II) may be attributed to hydrogen bonds between the ether oxygen of POE and the hydroxy group of the acid. The concentration of the proton

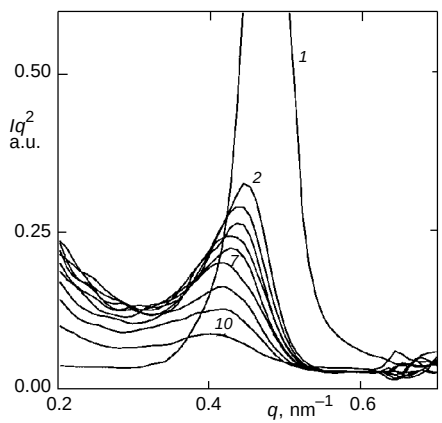

FIG. 8

Temperature changes of SAXS curves of 1st order SAXS reflection of HO-POE–benzoic acid mixture (w_{POE} = 0.85). *1* 20 °C, *2* 39 °C, *3* 40 °C, *4* 41 °C, *5* 42 °C, *6* 43 °C, *7* 44 °C, *8* 45 °C, *9* 46 °C, *10* 47 °C

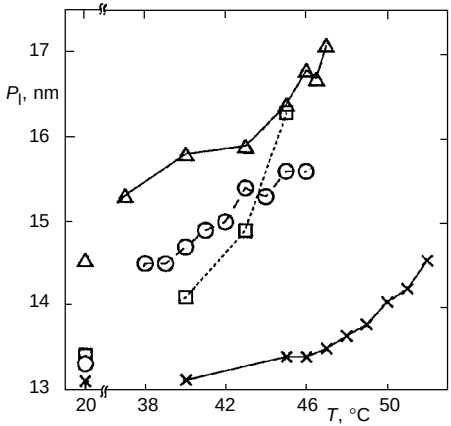

FIG. 9

Temperature changes of long period (P_l) in: MeO-POE–benzoic acid, w_{POE} = 0.84 (Δ); HO-POE–benzoic acid, w_{POE} = 0.85 (○); HO-POE–glutaric acid, w_{POE} = 0.80 (□); neat HO-POE (×)

donor groups in glutaric acid is twice as high as in benzoic acid, and therefore the χ parameter is more negative in mixtures of the former. 1,2-Diphenylethane can be considered a dimer of toluene. The interaction parameter of toluene with POE was measured by inverse gas chromatography[25]; the values of various authors range from 0.27 to 0.39 at 70 °C. The χ-parameter of 1,2-diphenylethane, if related to a volume corresponding to the molar volume of toluene, is 0.20, i.e. lower than χ of toluene. This result can be interpreted, following the Flory–Patterson equation-of-state theory, as a consequence of the smaller difference in free volumes in the dimer–polymer mixture, compared to the difference in monomer–polymer systems.

The POE 2000 forms in the solid state highly ordered structure of stacked extended-chain crystalline lamellae of practically uniform thickness with narrow amorphous surfaces consisting of the chain ends. Such structure gives several orders of reflection on SAXS curves (Fig. 5). When the mixtures are in the region with single liquid phase, the penetrating diluent not only increases the mean distance of lamellae, but also disturbs interlamellar periodicity (disappearance of higher-order SAXS reflections) by inhomogeneous swelling of the lamellar stacks. The increase of mean lamellar distance in pure POE in the neighbourhood of its melting point is much smaller (Fig. 9) and distortion of interlamellar periodicity is not so high as in the case of mixtures. This difference is associated with relatively high content of liquid phase in the mixtures. On the contrary, in pure POE, only small amount of liquid phase could exist at temperatures close to the melting point, where partial melting of crystalline lamellae can occur.

The increase of the long period of mixtures with increase in temperature (Fig. 9) gives an idea on the behaviour of the semicrystalline phase when cooled below the crystallization temperature of POE: The diluent is gradually expelled from the interlamellar layers and, below the eutectic crystallization temperature, it is virtually absent from the stacked-lamellae systems (Table III). This is a remarkable conclusion, if we realize that interlamellar layers are believed to be amorphous (i.e. swellable) and that both molten glutaric and benzoic acids enter into strong thermodynamic interaction with POE.

We have found that the calorimetric heat of fusion ΔH_{2u} is the proper parameter in the description of the POE 2000 melting branch by Eq. (*2*). As long as the amorphous portion of the polymer is constituted by interlamellar layers only, the enthalpy change ΔH_{2u} = 7.5 kJ/mol represents the *P*-th part of the enthalpy of transfer of one mol of chains from the lamellar system to the pure polymer melt, *P* being the degree of polymerization. The dominant part of this enthalpy change originates in the melting of crystalline stems, the contribution of the terminal parts of the chains being marginal. Our conclusion on ΔH_{2u} is empirical. A thermodynamic theory describing the fusion of the stacked lamellae in presence of diluent should take into account the effect of swelling of the interlamellar layer and would probably require more detailed information on the properties of this layer.

Many pairs of chain ends which are present in the interlamellar layers are likely to be linked by hydrogen bonds in POE terminated by hydroxy groups, but not in MeO-POE. The different character of interlamellar layers could be reflected in different behaviour of the mixtures with benzoic acid. However, X-ray and DSC measurements of MeO-POE gave essentially the same results in mixtures as those of HO-POE. Different long periods of MeO-POE and HO-POE (Fig. 9; 20 °C) in the solid-state mixtures are practically the same as for neat polymers and they are probably associated with differences in structure parameters of polymer chains only. The resulting change of long periods during heating in the temperature range where one phase is liquid is comparable for both mixtures (difference is 0.4 nm). Thus, our results bring evidence that the difference in hydrogen-bonding ability of end groups is virtually irrelevant as far as the aspects of polymer–liquid mixing, treated in this discussion, are concerned.

The financial support of the Grant Agency of the Czech Republic (Grant No. 106/95/0670) and of the Grant Agency of the Academy of Sciences of the Czech Republic (Grant No. 450 12) is gratefully acknowledged.

REFERENCES

1. Gryte C. C., Berghmans H., Smets G.: J. Polym. Sci., Polym. Phys. Ed. *17*, 1295 (1979).
2. Wittmann J. C., Manley R. S. J.: J. Polym. Sci., Polym. Phys. Ed. *15*, 2277 (1977).
3. Hager S. L., Macrury T. B.: J. Appl. Polym. Sci. *25*, 1559 (1980).
4. Bogdanov B., Mihailov M.: J. Polym. Sci., Polym. Phys. Ed. *23*, 2149 (1985).
5. Farina M., Di Silvestro G., Grassi M.: Makromol. Chem. *188*, 1041 (1979).
6. Smith P., Pennings A. J.: Polymer *15*, 413 (1974).
7. Hodge A. M., Kiss G., Lotz B., Wittmann J. C.: Polymer *23*, 985 (1982).
8. Smith P., Pennings A. J.: J. Polym. Sci., Polym. Phys. Ed. *15*, 523 (1977).
9. Smith P., Alberda van Ekenstein G. O. R., Pennings A. J.: Br. Polym. J. *9*, 258 (1977).
10. Wittmann J. C., Manley R. S. J.: J. Polym. Sci., Polym. Phys. Ed. *15*, 1089 (1977).
11. Wunderlich B.: *Macromolecular Physics*, Vol. 3, Chap. 8. Academic Press, New York 1980.
12. Buckley C. P., Kovacs A. J.: Prog. Coll. Polym. Sci. *58*, 44 (1975).
13. Laggner P., Mio H.: Nucl. Instrum. Methods Phys. Res., A *323*, 86 (1992).
14. Petkov V., Bakaltchev N.: J. Appl. Crystallogr. *23*, 138 (1994).
15. Glatter O.: J. Appl. Crystallogr. *7*, 147 (1974).
16. Mandelkern L.: *Crystallization of Polymers*, Chap. 3. McGraw–Hill, New York 1964.
17. Flory P. J.: *Principles of Polymer Chemistry*, p.508. Cornell University Press, Ithaca 1953.
18. *Beilsteins Handbuch der organischen Chemie*, 4th ed., Vol II, Part 2, p. 1686. Springer, Heidelberg 1961
19. *Beilsteins Handbuch der organischen Chemie*, 4th ed., Vol. XI, Part 1, p. 363. Springer, Heidelberg 1961.
20. Vecera M., Gasparic J., Churacek J., Borecky J.: *Chemicke tabulky organickych sloucenin*. SNTL, Praha 1975.
21. Cheng S. Z. D., Wunderlich B.: J. Polym. Sci., Polym. Phys. Ed. *24*, 595 (1986).
22. Balta-Calleja F. J., Vonk C. G.: *X-Ray Scattering of Synthetic Polymers*, p.272. Elsevier, Amsterdam 1989.

23. Alexander L. E.: *X-Ray Diffraction Methods in Polymer Science*. Wiley-Interscience, New York 1969.
24. Terrisse J., Markis A., Skoulios A.: Makromol. Chem. *119*, 219 (1968).
25. Galin M.: Polymer *24*, 865 (1983).